



44TH TURBOMACHINERY & 31ST PUMP SYMPOSIA
HOUSTON, TEXAS | SEPTEMBER 14 – 17 2015
GEORGE R. BROWN CONVENTION CENTER

COUPLED TORSIONAL AND LATERAL ANALYSIS FOR THE DETERMINATION OF THE DAMPING OF THE FIRST TORSIONAL MODE OF SYNCHRONOUS MOTOR DRIVEN COMPRESSOR TRAINS

Jean-Claude Pradetto

Head of In Service Development (ISD)
MAN Diesel & Turbo Schweiz AG
Zürich, Switzerland



Jean-Claude Pradetto is the Head of the In Service Development group of MAN Diesel & Turbo Schweiz AG in Zurich, Switzerland. He is responsible for trouble shooting issues and for the improvement of the turbocompressors.

Before joining the Calculation and Development department of MAN Diesel & Turbo in 2012, he worked as development engineer for Sulzer Turbo and as consulting engineer for Delta JS in Zurich. He has more than 25 years of experience in Rotordynamics and in the field of magnetic bearing applications.

Jean-Claude Pradetto has a diploma (Mechanical Engineering, 1988) from the Swiss Federal Institute of Technology in Zurich.



Urs Baumann is the Manager of the Calculation and Development department of MAN Diesel & Turbo Schweiz AG in Zurich, Switzerland. His responsibilities include the aerodynamic as well as the mechanical development and improvement of turbocompressors and associated components, as well as the implementation and maintenance of test stands and

analytical tools needed to fulfill this task. His department comprises also a Product Development Group mainly focussing on high-speed motor driven, magnetically suspended compressors. He is the owner of several patents related to high pressure compression and high-speed oil-free motor compressors.

Before joining MAN Diesel & Turbo in 1996, Mr. Baumann worked for Sulzer Innotec, the Corporate Research and Development Center. For several years he was in charge of the machinery dynamics group which is responsible for the development, design improvement and trouble shooting on a wide range of Sulzer products.

Urs Baumann has a diploma (Mechanical Engineering, 1987) from the Swiss Federal Institute of Technology in Zurich.

ABSTRACT

This paper deals with the damping ratio D of the 1st torsional mode of synchronous motor driven compressor trains. The

Urs Baumann

Manager Calculation & Development
MAN Diesel & Turbo Schweiz AG
Zürich, Switzerland

damping ratio is a crucial parameter for the torsional start-up analysis and for the lifetime calculation of the shafts.

At the start-up, a synchronous motor runs in an asynchronous mode and generates oscillating torques with two times the slip frequency. The frequency of the pulsating torques decreases with the rotor speed and the resonance with the 1st torsional mode of the shaft train cannot be avoided. In resonance the shafts and couplings are highly loaded and the shaft stresses exceed the fatigue limit. Therefore, the number of the admissible starts is normally limited.

The magnitude of the torques at resonance (and by consequence the shaft stresses) is strongly dependent on the damping ratio of the train's fundamental mode. For the analyses, the assumed damping is normally based on the compressor manufacturer's experience, which is built up from several measurements formerly done at similar trains. The data are in agreement with the commonly used standard value for geared trains, which ranges from $D=2\%$ to $D=5\%$.

In the first section of the paper, two measurements are presented, which were recently performed at two air compressor trains. The trains were of the same arrangement, but with different sizes of the components. The torques were measured during the start-up with strain gauges at the low speed couplings. The fundamental mode's damping was determined by curve-fitting with a linear one-mass model. For both trains, the identified damping was considerably higher than expected. Further on, non-linear effects were observed at resonance.

In a second section the paper deals with coupled torsional and lateral (T&L) analyses. The torsional and lateral degrees of freedom of the shaft train model were coupled via the gear. The damping in resonance was determined with an eigenvalue analysis of the coupled system. Herewith, it was attempted to explain at least the linear portion of the identified damping and, respectively, the contribution of the gear's fluid film bearings to the effectively measured damping. The calculations confirmed the higher damping ratio for the two measured trains.

The investigations were extended to several compressor trains of different sizes. It was observed that the damping varies depending on the actual inertia and stiffness proportions of the train components. The deviation from the usually employed standard damping can be either higher or lower values.

The eigenfrequency of the 1st torsional mode was found to be a practical parameter for the first screening of similar comp-

ressor trains, with regard to the mode's damping ratio.

INTRODUCTION

At the start-up of synchronous motor driven compressor trains, the motor operates in an asynchronous mode until the operating speed is reached and the motor is synchronized to the electrical line frequency. In the asynchronous mode, the motor generates oscillating torques, which frequency is two times the slip frequency between the rotating speed and the line frequency. The frequency of the oscillating torques decreases with increasing speed and the torque excitation inevitably becomes resonant with torsional modes of the shaft train. The resonance with the 1st or fundamental mode is the one of most concern. The shafts and couplings are highly loaded when this resonance is passed through and typically the admissible number of starts of such trains is limited.

The subject of synchronous motor driven turbomachinery is thoroughly discussed by Corbo (2002). The calculation of the torque load at start-up and the shafts' lifetime is part of the standard torsional analysis also required by API 617 (2002). The analysis is presented in API 684 (2005).

The results are strongly dependent on the damping ratio D (which is assumed for the 1st torsional mode), on the magnitude of the pulsating torques and on the rate of acceleration when running through the resonance. Reliable data for the pulsating and average motor torques is obtained from the motor manufacturer. The average motor torque determines the acceleration of the rotors. For the system's damping, the data is based on the compressor manufacturer's experience and, respectively, on former measurements for similar applications. The authors company's standard practice is the assumption of D=3%.

The torsional analysis for two specific compressor trains revealed, that the load on the shafts during the start-up was much too high. Therefore, it was proposed to retrofit the trains with torque limiting devices, e.g. slipping clutches. The measurement of the torque load during the start-up should provide the basis for their design. The measurements were carried out for both compressor trains. The measured torques turned out to be much lower than predicted. Consequently the torque limiting devices were not required.

Based on the measured data, it was recognized that the lower than expected torques are due to the system's damping, which is considerably higher than assumed. Moreover, it was found that the damping clearly varies from train to train. An attempt to explain the measurement results was made by calculating the damped eigenvalues of the torsionally and laterally coupled system. With the coupled torsional and lateral (T&L) analysis, the gear's bearings influence on the damping of the torsional modes is considered. The gear bearings' influence was investigated by Viggiano and Wattering (1994) with a simplified model for the torsional-lateral motion of the gear shafts. The T&L analyses here presented are based on detailed models of the shaft trains and of the bull gear and pinion shaft's bearings.

The calculations were made for a variety of compressor trains with identical arrangement and with the same type of gear and bearings as for the measured trains.

ASYNCHRONOUS START OF A SYNCHRONOUS MOTOR

The motor torque characteristics for the asynchronous start-up of a synchronous motor are normally provided by the motor manufacturer. As an example, the characteristics for the first train measured (train A), are shown in Figure 1.

The acceleration of the rotors and the resulting run up time result from the difference between the average motor torque "A" and the compressor's counter torque "C". The frequency "F" of the pulsating motor torque "P" is two times the slip frequency between the line frequency and the rotating speed. For a 4-pole (or half-speed motor), it can be written as follows:

$$F = 2 \cdot (f_{line} - 2 \cdot N / 60) \quad (1)$$

$$\begin{aligned} F &= \text{Excitation frequency of the pulsating torques (Hz)} \\ f_{line} &= \text{Electrical line frequency (50Hz or 60Hz)} \\ N &= \text{Rotor speed (rpm)} \end{aligned}$$

At zero rotor speed the excitation frequency F is twice the electrical line frequency, i.e. 120Hz for a 60Hz and 100Hz for a 50Hz grid. During run up, the frequency decreases linearly with the rotor speed and reaches 0Hz at full (or synchronous) speed.

In Figure 1 the red dashed lines mark the eigenfrequencies of the lowest three torsional modes. The resonances of the excitation frequency F with these modes occur at the intersection points of the dashed red lines and line "F". In the figure the resonances are marked with red circles. For the 1st mode, the speed (1'175rpm) and the magnitude of the pulsating torque (0.41pu) at resonance are also marked with red circles.

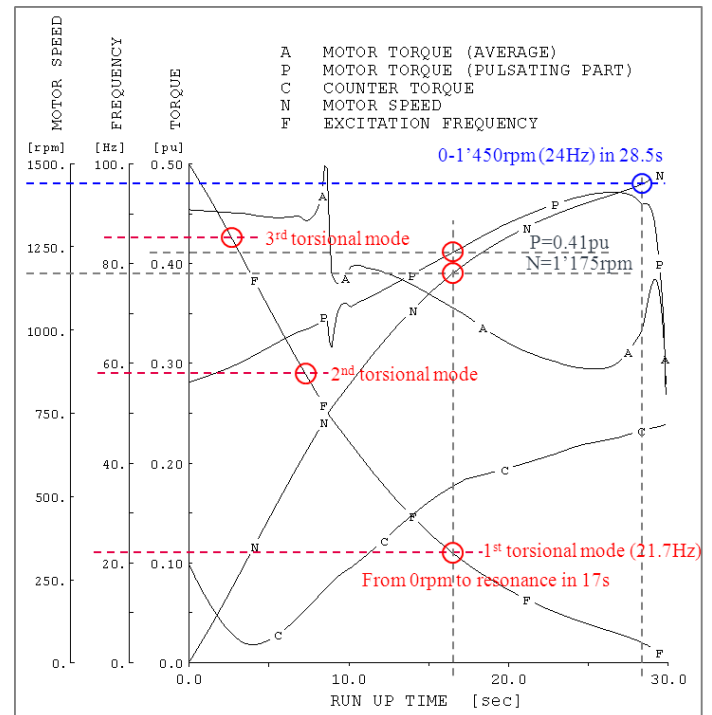


Figure 1. Motor Start-up Characteristics (Train A)

DESCRIPTION OF THE INVESTIGATED SHAFT TRAINS

The arrangement of the investigated trains consists of the air compressor, a double helical gear box and the synchronous motor. The shafts are connected with two flexible couplings. The arrangement for these applications is always identical, the size of motor, compressor, gear box and couplings varies according to the rated power.

Measurements were done at two compressor trains of different sizes. The main data of these are summarized in Table 1. The compressor of train A is equipped with three impellers, the one of train B with four.

Table 1. Main Data of the Air Compressor Trains

	Train A	Train B
Compressor Size	“80-3”	“125-4”
Nominal Power	18’300 HP (13’650 kW)	33’700 HP (25’150 kW)
Nominal Speed (LS/HS)	1’500 / 6’828 rpm	1’500 / 4’537 rpm
Nominal Torque (LS)	769’100 lbf-in (1 pu) (86’899 Nm)	1’417’100 lbf-in (1 pu) (160’110 Nm)
Gear Ratio	4.552 (=132/29)	3.024 (=124/41)

PREDICTED START-UP BEHAVIOUR

The start-up of a train is simulated with a transient torsional analysis. The main results of this analysis are the torque distribution in the shafts and couplings, as well as the run-up time. The time responses of the torques are plotted for the relevant shaft sections. The maximum torque amplitudes occur, when the pulsating motor torques are in resonance with the 1st torsional (or fundamental) mode of the train. The frequency of this mode is calculated with an eigenvalue analysis. The amplitude and the number of the torque peaks in resonance determine the admissible number of starts.

In the following, the analysis results are presented for the two trains, where the torque measurements were performed.

Train A

The lowest three mode shapes for train A are shown in Figure 2. The calculated frequency of the 1st undamped torsional mode is $f_0=21.7\text{Hz}$.

The calculated time response of the torque at the low speed coupling is shown in Figure 3. The response is calculated with $D=3\%$ damping ratio for the 1st mode and $D=0.7\%$ for the higher ones. The time t_0 to reach the resonance, the run-up time and the mean torque are summarized in Table 2, the peak torques in resonance in Table 3.

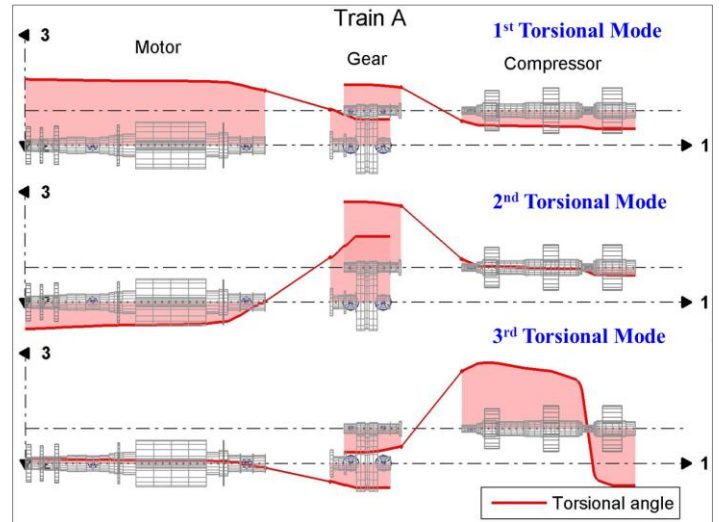


Figure 2. Shape of the Lowest Three Torsional Modes (Train A)

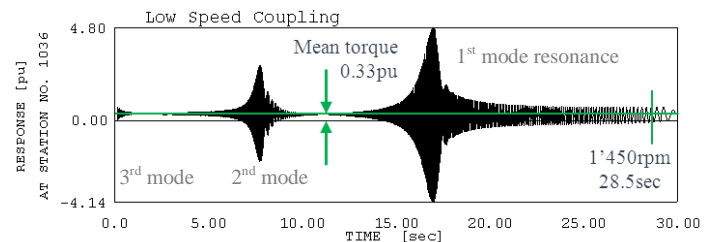


Figure 3. Calculated LS Coupling Torque at Run-up (Train A)

Train B

The shape of the 1st torsional mode is shown in Figure 4. The shapes of the 2nd and 3rd modes are similar to the ones of train A and are therefore not shown here. The calculated undamped eigenfrequency of the 1st mode is $f_0=20.8\text{Hz}$.

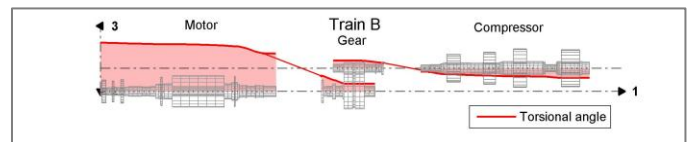


Figure 4. Shape of the 1st Torsional Mode (Train B)

The time response of the torque at the low speed coupling of train B is shown in Figure 5. The time t_0 to reach the resonance, the run-up time and the mean torque are summarized in Table 4. The peak torques in resonance are summarized in Table 5. For the calculation of the response, the same damping ratios were assumed as for train A.

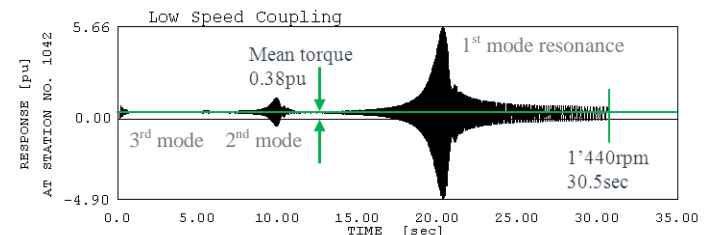


Figure 5. Calculated LS Coupling Torque at Run-up (Train B)

MEASUREMENTS

The torque load in the shafts was measured by applying two strain gauges at the LS coupling spacer. The strain gauges were mounted in a 180° configuration (i.e. opposite to each other). They were connected as two Wheatstone half-bridges to a full bridge. This connection has the advantage, that the influence of a shaft bending is eliminated. The strain gauge signal was transmitted by telemetry. A transmitter sent the modulated radio signal via antenna from the rotating system to the stationary receiver. The power for the transmitter was supplied from an electromagnetic field. Hence, no batteries had to be fixed at the rotating shaft. Finally, in the data acquisition box the frequency signal was de-modulated and converted to an analogue, torque proportional voltage signal.

The speed was measured with an inductive sensor placed at the coupling. The purpose of the additional speed measurement was to get synchronous speed and torque signals. The signals were stored in the data acquisition box.

The measurement arrangement is shown in Figure 6.

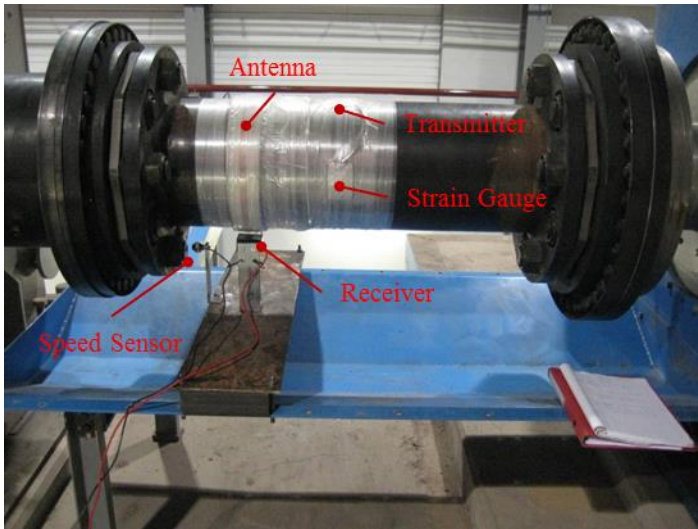


Figure 6. Measurement arrangement at the low speed coupling

The electrical parameters such as the mains voltage and currents were recorded with a low sampling rate. The currents and voltages at the motor clamps and the effective motor torques, respectively, were not directly measured. The reliability of the motor data was checked by the plausibility of the run-up time and mean driving torque.

Train A

The torque measured during the run-up of train A is shown in Figure 7 together with the rotor speed. The highest torque peak occurs, when the exciting motor torque is in resonance with the 1st torsional mode of the shaft train. The resonances with the 2nd and 3rd torsional mode are visible in the lower speed range, the peaks are small. The shock torque loads, which can be seen after the full speed is reached, are due to the synchronization of the motor with the electrical line frequency.

Some characteristic data, as the time t_0 to reach the main resonance, the time t to reach full speed and the mean torque during the run-up are summarized in Table 2, where they are

compared with the predicted data.

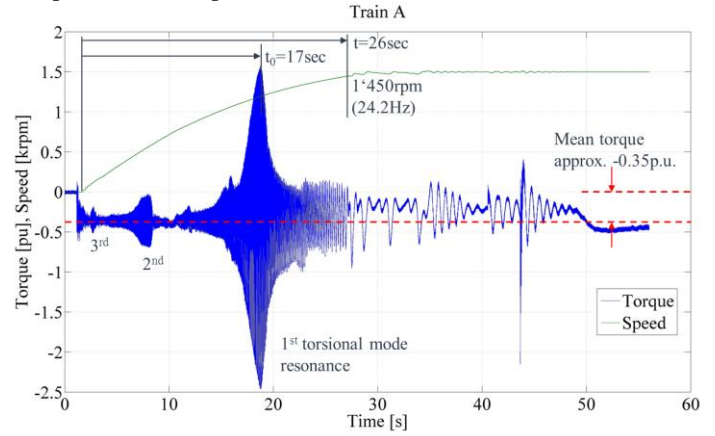


Figure 7. Measured Coupling Torque during Run-up (Train A)

Table 2. Characteristic Run-up Data (Train A)

	Time t_0 to Resonance	Run-up Time (0-1'450rpm)	Mean Torque (Static)	1 st TNF f_0
Predicted	17sec	28.5sec	+0.33pu	21.7Hz
Measured	17sec	26.0sec	-0.35pu	21.2Hz

The data in Table 2 show a good correlation between the measurements and the predictions in terms of total run-up time, mean torque and time to reach the resonance. This leads to the conclusion that the motor behavior given by the motor manufacturer is correct.

However, looking at the maximum torque peak, it can be seen that the measured resonance peak is much smaller than the predicted one. The comparison of the peak-torques is shown in Table 3. The measured peak-to-peak torque amplitude is 2.02pu, whereas the predicted one was 4.47pu. Thus, there is a clear deviation of more than a factor of two between measurement and calculation.

Table 3. Peak Torque in the LS Coupling (Train A)

	Tmax / Tmin	T-Amplitude
Predicted, D=3%	+4.80 / -4.14pu	4.47pu
Predicted, D=6.5%	+2.54 / -1.89pu	2.22pu
Measured	-2.46 / +1.57pu	2.02pu

The torsional analysis was re-run with an increased damping ratio for the 1st torsional mode. It was found that a damping ratio D=6.5% would be necessary to bring down the peak-to-peak-torque amplitude to the measured level.

Train B

The torque measurement was repeated for a larger train (train B). The measured torque and rotor speed are shown in Figure 8. Here the torque is plotted as envelope, slightly different from the measured data for train A. Again, two small resonances with the 2nd and 3rd torsional mode of the shaft train

are visible in the lower speed range, which are followed by the main resonance with the 1st mode.

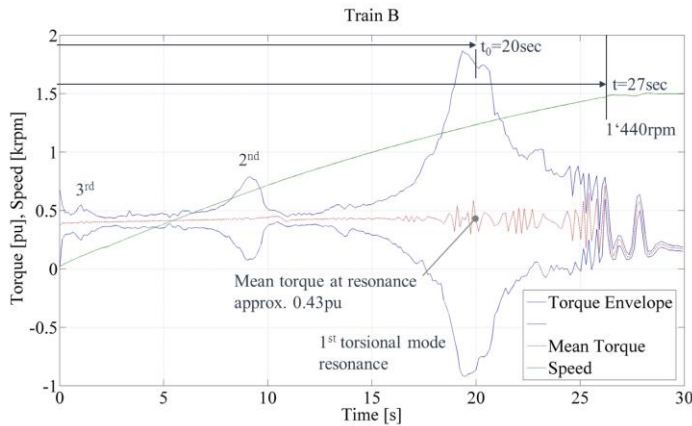


Figure 8. Measured Coupling Torque at Run-up (Train B)

In Table 4 the time t_0 to reach the main resonance, the time to reach full speed, as well as the mean torque during the run-up are summarized and compared with the predicted data. As for train A, there is a quite good correlation between measurement and prediction regarding these values.

Table 4. Characteristic Run-up Data (Train B)

	Time t_0 to Resonance	Run-up Time (0-1'440rpm)	Mean Torque (Static)	1 st TNF f_0
Predicted	20sec	30.5sec	+0.38pu	20.8Hz
Measured	20sec	27sec	+0.43pu	18.7Hz

The comparison of the measured and predicted peak-torques is shown in Table 5. Also for train B, the maximum torque peak in resonance is much smaller than predicted and only the assumption of a very high damping ratio of $D=11\%$ for the 1st torsional mode would result in almost comparable peaks.

Table 5. Peak Torque in the LS Coupling (Train B)

	Tmax / Tmin	T-Amplitude
Predicted, $D=3\%$	+5.66 / -4.90pu	5.28pu
Predicted, $D=5.0\%$	+3.71 / -2.97pu	3.34pu
Predicted, $D=11.0\%$	+1.94 / -1.19pu	1.57pu
Measured	+1.87 / -0.92pu	1.40pu

IDENTIFICATION OF THE MEASURED DAMPING

A one-mass system was used for the detailed assessment of the resonance peak. With this model, the eigenfrequency of the 1st torsional mode and the damping ratio D could be determined by curve-fitting the measured torque curve. The model is linear and considers the torque reduction and frequency shifting effects due to the acceleration. The model is described in Gasch et al. (2005). The input (or model) parameters for the fitting are the following:

A = Excitation amplitude [lbf-in] ([Nm])

Λ = Acceleration of the pulsating torque frequency [$1/s^2$]

D = Damping ratio [-]

With the proper selection of these parameters, the calculated response torque was iteratively adapted to the measurement. In the one-mass model, the excitation amplitude A , as well as the acceleration Λ are constant parameters. In reality, these parameters are varying during the start-up. The acceleration Λ is the second derivative of the pulsating torque frequency, which is related to the measured speed according to Equation (1).

Identification for Train A

In the upper half of Figure 9, the time range of the run-up, which was used for the curve-fit is shown. The plot is a zoom of the measurement already shown in Figure 7. In the lower half of the figure the rotor speed, the frequency of the excitation and the acceleration of the excitation are plotted. The (constant) acceleration value used for the fitting is marked with a star.

In Figure 10 the curve-fits for an assumed damping ratio of $D=3\%$ and $D=6.5\%$, respectively, are shown. The blue lines represent the measured torques, the red lines show the envelopes of the torques, which result from the calculations with the one-mass model. The torques are drawn versus the ratio of the excitation frequency to the identified eigenfrequency. The eigenfrequency was identified as $f_0=21.2\text{Hz}$. It fits very well with the prediction.

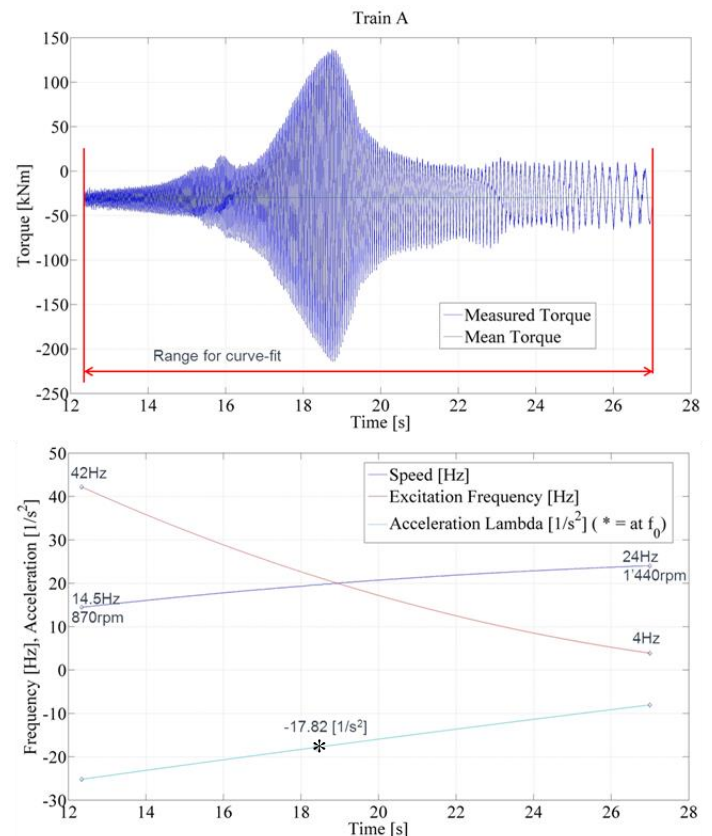


Figure 9. Speed, Excitation Frequency and Acceleration

The plots show that the mode's damping is clearly higher than 3%. First of all, because the peak torque is obviously smaller than calculated, but also, because the typical acceleration effect (circle in Figure 10) is not visible.

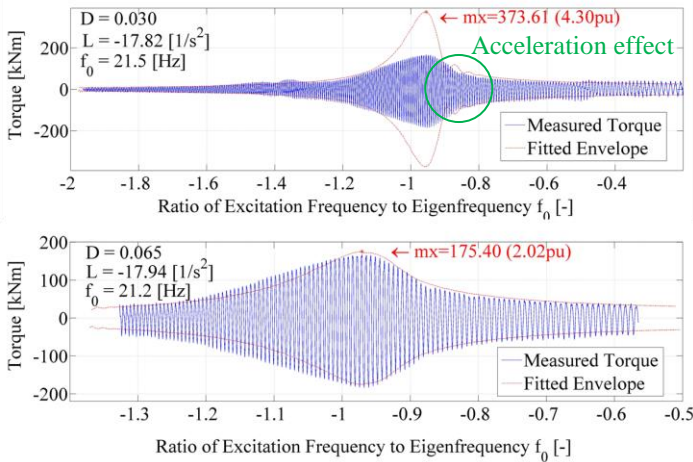


Figure 10. Curve-Fit, D=3% and D=6.5% (Train A)

The curve-fit for D=6.5% shown in the lower half of the figure matches the measurement quite well in the range after the resonance is crossed. However, in the range before the resonance is reached, the fit is rather poor. Obviously, the torque cannot be approximated over the full range by this simple linear model.

Identification for Train B

The curve-fits for train B were done in a similar way as for train A. The time range used is shown in Figure 11. The corresponding rotor speed, the frequency of the excitation and its acceleration are shown in Figure 12. The curve-fits for the assumed damping ratios of D=3%, 5% and 11% are shown in Figure 13. The identified eigenfrequency f_0 is between 18.6Hz and 18.8Hz. This corresponds quite well to the prediction.

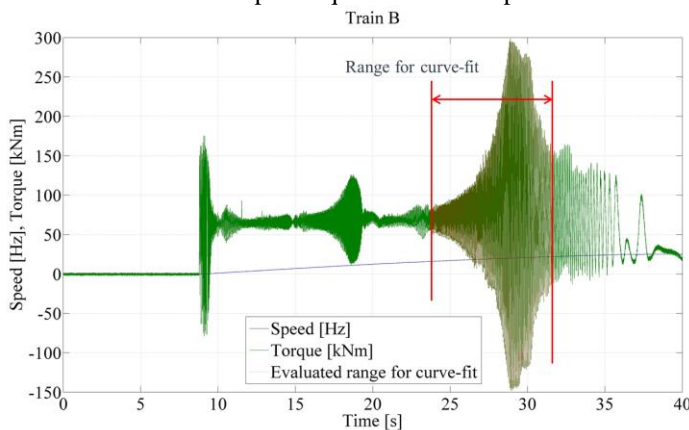


Figure 11. Range for Curve-Fit (Train B)

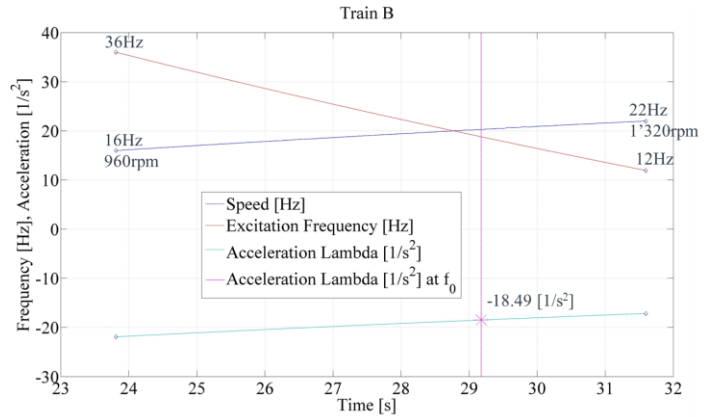


Figure 12. Speed, Excitation Frequency and Acceleration

The curve-fits shown in Figure 13 demonstrate that the train B damping must also be considerably higher than 3%. Interesting is the curve-fit for D=5%. Here, the calculated torque envelope shows the typical effect of the accelerated crossing of the resonance, which can also be seen for the measured torque. However, for this fit and even for the fit with D=11%, the low measured peak cannot be reflected. It appears that in resonance there are non-linear effects, which limit the torque amplitude and further increase the apparent (linear) damping.

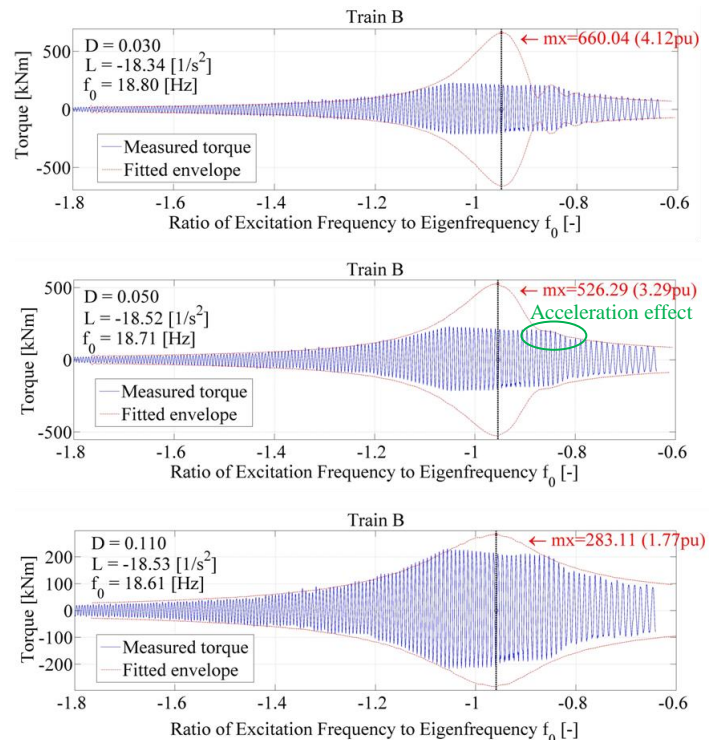


Figure 13. Curve-Fit, D=3%, D=5% and D=11% (Train B)

As a conclusion, it can be stated, that for both measurements, the identified damping is markedly higher than normally assumed for the torsional analysis. Further on, it differs from train to train.

COUPLED TORSIONAL AND LATERAL ANALYSIS

It was attempted to calculate the gear's contribution to the damping of the 1st torsional mode, by means of a coupled Torsional and Lateral (T&L) analysis including a damped eigenvalue analysis. The damping arises from the bull gear and pinion shafts' fluid film bearings, which dampen the lateral motion of the shafts. It is transmitted to the torsional motion via the gear mesh.

The analysis is linear. Therefore, only the linear damping portion can be determined. Additional influences such as non-linear effects of the gear and structural damping (friction in the rotor components, e.g. in the flexible couplings) are not considered. By consequence, the calculated damping ratio is basically lower than in reality.

FE Model

The rotors are modeled with finite elements. The cross sections of the shafts are specified by their stiffness and mass diameters. Rigid rotor components (e.g. impellers, fans and coupling hubs) are modeled as discrete masses. The FE model of train A is shown in Figure 14. The silhouette of the shaft train represents the mass diameter.

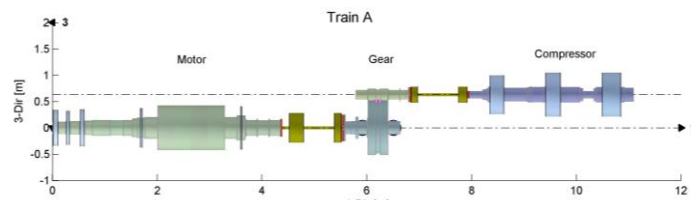


Figure 14. FE Model of the Shaft Train (Train A)

The coupling effect in the gear is modelled by connecting the gear teeth with a spring. The toothing itself is modelled with rigid elements; the spring is aligned with the contact force of the teeth. For the spring rate, a relatively high value of $5.71 \cdot 10^7$ lbf/in ($=10^{10}$ N/m) was assumed. The spring rate has little impact on the eigenvalues of the 1st torsional mode, as long as it is an order of magnitude higher than the effective tooth stiffness (or higher) and the coupling effect is assured. With the stiff connection, the torsional oscillation of the bull gear and pinion shafts is coupled with their lateral motion. The gear's model is shown in Figure 15.

More general details regarding the FE-model and the used rotordynamic software are described in Schmied, et al. (2007).

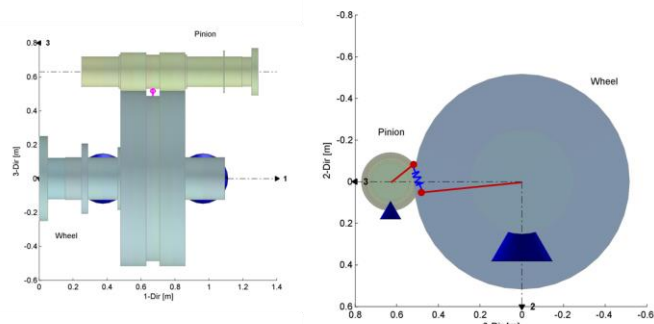


Figure 15. Model of the Gear and of the T&L Coupling

For all investigated shaft trains, the gear is arranged “up-mesh” (load on the pinion bearing points upwards).

Bearing Data

The fluid film bearings of the gears are all of the same type. The actual size depends on the machine's size. The bull gear bearings are cylindrical, the pinion bearings of the double- or lemon-offset type. The geometries for shaft train A are shown in Figure 16. The main bearing data for train A and B are summarized in the Tables 6 and 7.

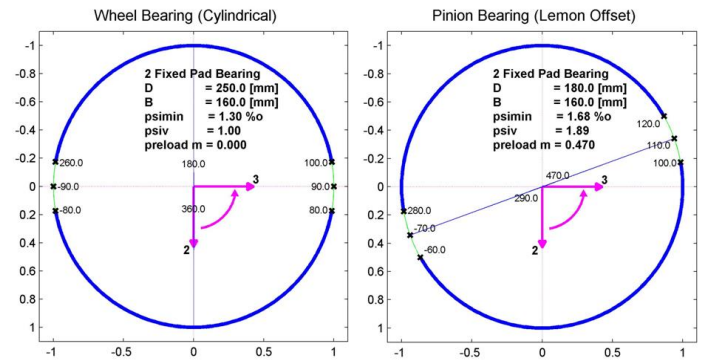


Figure 16. Geometry of the Bull Gear and Pinion Bearings (Train A)

Table 6. Main Data of the Gear Bearings (Train A)

Shaft Train A	Bull Gear	Pinion
Bearing Type	Cylindrical	Lemon Offset
Diameter, D	250mm	180mm
Relative Width, B/D	0.64	0.89
Relative Clearance, Ψ_m	1.30‰	1.68‰
Preload	0.0	0.47
Circumferential Velocity	19.6m/s	64.4m/s
Specific Load (Nominal)	21.0bar	29.2bar

Table 7. Main Data of the Gear Bearings (Train B)

Shaft Train B	Bull Gear	Pinion
Bearing Type	Cylindrical	Lemon Offset
Diameter, D	315mm	250mm
Relative Width, B/D	0.63	0.90
Relative Clearance, Ψ_m	1.30‰	1.50‰
Preload	0.0	0.45
Circumferential Velocity	24.7m/s	59.4m/s
Specific Load (Nominal)	23.8bar	26.7bar

The relative width and the relative clearance of the bull gear bearings are identical, whereas the pinion bearings are of the same relative width, but they have a slightly different relative clearance.

Eigenvalues and Mode Shapes

The damping ratio, the eigenfrequency and the shape of the 1st torsional mode result from a damped eigenvalue analysis. The analysis is based on constant bearing stiffness and damping coefficients. The coefficients result from the linearization of the bearing force around the static shaft position, which is given by the rotor speed and the load on the bearings. The gear load and the rotor weight were considered for the calculation of the bearing load.

The eigenvalues were calculated for 80% of the nominal speed. This is approximately the resonance speed with the 1st torsional mode; it is almost identical for the investigated trains. The load was varied in three steps, assumed were 2%, 10% and 35% of the nominal gear load.

The mode shape of train A is shown in Figure 17.

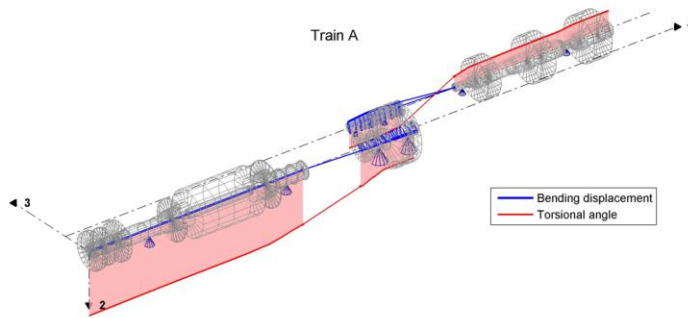


Figure 17. Mode Shape of the Coupled 1st Torsional Mode (Train A)

In the plot, the torsional twist of the shafts is shown in red, the lateral displacement in blue. The twist of the low speed shafts is scaled with half the pitch diameter of the bull gear mesh, analogously the twist of the high speed shafts with half the pitch diameter of the pinion mesh. Herewith, the torsional and lateral displacements can be compared. The coupling of the torsional and lateral motion in the gear is clearly visible in the plot.

In Figure 18 the calculated damping ratios for the shaft trains A and B are plotted vs. the load. The damping ratios decrease with increasing load. For all loads the damping for train B is higher than for train A.

The results basically confirm the measurements, in terms of train B being better damped than train A. Quantitatively the calculated results fit best for a gear load in the range of 10% of the nominal load. Here the calculated damping ratios are $D=3.7\%$ for train A and $D=5.1\%$ for train B. The damping ratios are herewith lower than the identified ones, which are $D=6.5\%$ for train A and $D=11\%$ for train B.

For loads lower than 10%, the damping ratios are rather too high, in particular if one keeps in mind that further damping effects, which are not depicted in the T&L analyses, should be added to the results. Additional damping effects are the structural damping, as well as damping from non-linear effects, as seen in the measurements.

Further on, the calculated eigenfrequencies are $f=20.1\text{Hz}$ for train A and $f=19.1\text{Hz}$ for train B.

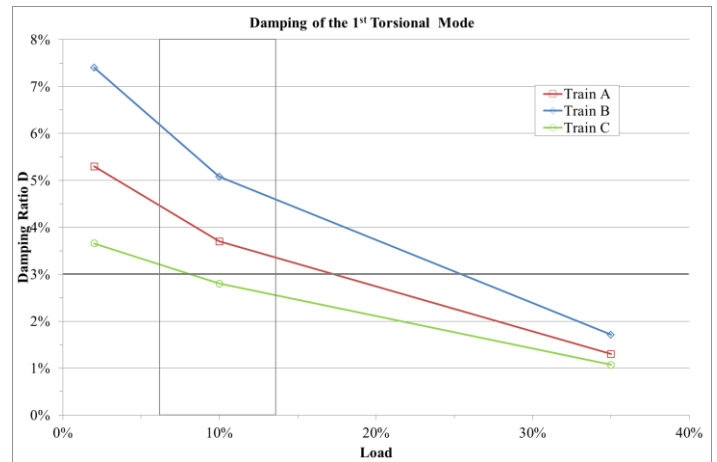


Figure 18. Damping Ratio for Varying Load (Train A, B, C)

The green line drawn in the plot in Figure 18 shows the resulting damping ratio for a shaft train C. This additional investigation was carried out, because the damping of shaft train C is well known from former measurements. At that time, the damping of the 1st torsional mode was identified to be $D=2.7\%$. The applied identification method was the same as presented in this paper.

The calculated damping ratio for 10% load is $D=2.8\%$. Hence, the calculation basically confirms the generally lower damping for train C. Again, the best match with the measurement is given for the load range around 10%, confirming the results for train A and B. Non-linear effects, as seen for train A and B, were not observed for train C.

The parameters, which influence the damping of the coupled 1st torsional mode are:

- The gear bearing coefficients
- The mode shape at the gear (coupling effect)

Both the bearing coefficients and the mode shape are load dependent. Strictly speaking, the mode shape also depends on the bearing coefficients. The influence of the mode shape on the damping can be expressed in terms of the coupling effect. In Figure 19 three zooms of the mode shapes at the gear of train A are shown. The pictures show the shapes for the investigated loads. Comparing the shapes, it is evident, that with increasing load the lateral displacements of the bull gear and pinion shafts decrease relative to their torsional twist, thus the coupling effect is reduced. The precondition for a significant damping transmission from the bearings to the torsional modes is, that the mode shapes are sufficiently coupled, i.e. an explicit torsional, as well as lateral motion of the gear shafts is needed. Hence, the effect of decreasing damping with higher load as seen in Figure 18 cannot solely be explained with the bearing coefficients alone, but also with a smaller coupling effect.

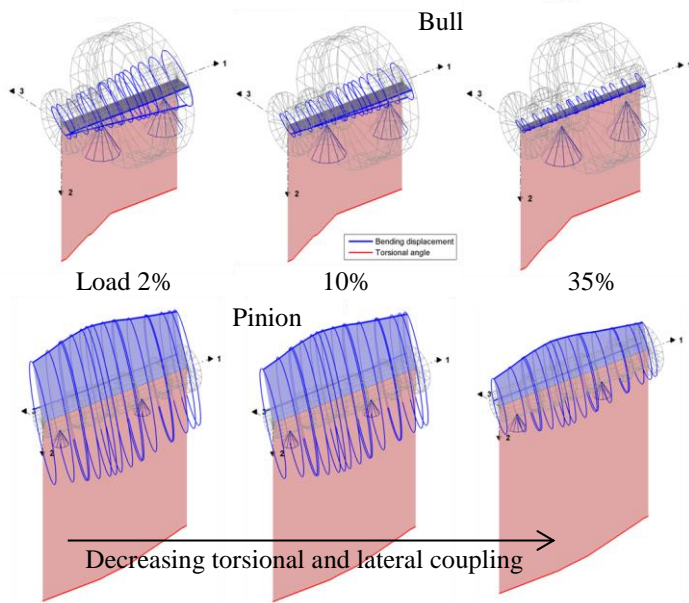


Figure 19. Mode Shapes of the Gear Shafts for Different Loads (Train A)

In reality, when the resonance is crossed at run-up, the gear load and herewith the load on the bearings is not well defined, because the pulsating response torque in resonance is much higher than the driving torque. This leads to a loss of contact at the driving side of the gear teeth surfaces and to a contact of the opposite surfaces. The effect is known as “torque reversal” or “backlash”. The assumption of bearing coefficients, which are linearized around the shaft position given by the static load and the speed are a clearly identified shortcoming of the linear T&L analysis method. Another approach would be to carry out a transient, non-linear run-up analysis, which considers the dynamic shaft position and lateral speed dependent bearing coefficients. However, for the investigated shaft trains it turned out, that the assumption of 10% gear load leads to results, which are conservative on one hand and fit quite well with the measurements on the other. The assumed load can therefore be interpreted as a “virtual load”, which leads to useful results.

Influence of Bearings and Coupling Effect

As shown in the diagram in Figure 18, the damping ratios for trains A, B and C are quite different and the question about the reason for these deviations comes up. Looking at the gear bearings, there is a small difference in the pinion bearing’s clearance between train A and B. Further on, the gear bearing’s geometry of train C is different compared with the one of all other investigated trains. The bull gear bearings are narrower ($B/D=0.5$) and the pinion bearings of a different type (4-lobe bearings, $B/D=1$). The clearances are also slightly different.

For train B, the calculations were repeated for exactly the same bearing geometries as used for train A and C. Herewith, the deviations of the damping ratios can be split into a portion, which can be explained by the different bearing geometries and a remaining portion, which is due to the mode shape itself and the different “coupling effects”, respectively. The results for 10% gear load are shown in Figure 20.

On the left side of the diagram, the damping for train B with the same bearings as train A is plotted and compared to the damping of train A. The difference is the damping portion due to the different “coupling effects”. The influence of the pinion bearing’s clearance (0.7 percentage point) is shown in the middle of the diagram.

On the right side of the diagram, the damping ratio for train B with the same bearings as train C is plotted. The totally 2.3 percentage point difference compared to train C can be explained with 1.2 percentage point from the different bearing geometries and 1.1 percentage point from the different “coupling effects”.

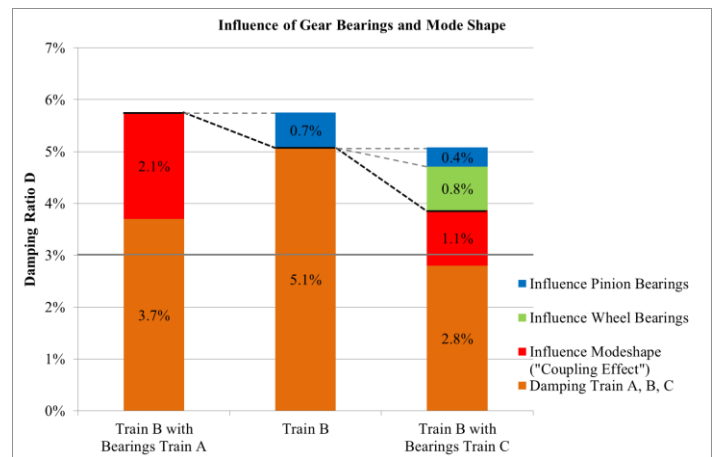


Figure 20. Influence of Bearings and Mode Shape, Load 10%

The parameters, which (besides the bearings) mostly affect the shape of the torsional modes and therefore have an influence to the mode’s damping, are discussed in the next section.

INFLUENCE OF THE MACHINE SIZES AND OF THE COUPLING STIFFNESS

The influence of the machine sizes and coupling stiffness on the damping of the 1st torsional mode was investigated by means of a parameter variation. The parameters varied were the motor and compressor inertia and the stiffness of the low and high speed couplings. The variations were carried out for a further train D, which is still of the same arrangement and with the same bearings as train A and B. The basic damping ratio for this train is $D=2.2\%$ for 10% gear load.

The results are presented in two figures. In Figure 21 the damping ratio D is shown for the variation of the coupling stiffness and motor inertia, while the compressor inertia is kept constant. Whereas in Figure 22 the analogous is shown for a constant motor inertia.

The black, dashed line corresponds to the relative inertia of the varied component, i.e. of the motor and of the compressor, respectively. The colored dots on this line mark the inertia, which was applied for the relative coupling stiffness variation. The results of the stiffness variation are shown by the families of colored curves. A continuous line is used for the low speed coupling and a dashed line for the high speed coupling variation.

According to the results, the motor inertia has the most

significant influence on the mode's damping. The damping is higher for a motor with low inertia. For the extreme case of a motor inertia reduced to 21% of the original value, the damping raises from the basic value $D=2.2\%$ up to $D=5.1\%$. Hence, the increase is more than twice the original value. The compressor inertia plays a minor role, as can be seen in Figure 22. The influence of the low speed coupling stiffness is generally higher than the one of the high speed coupling.

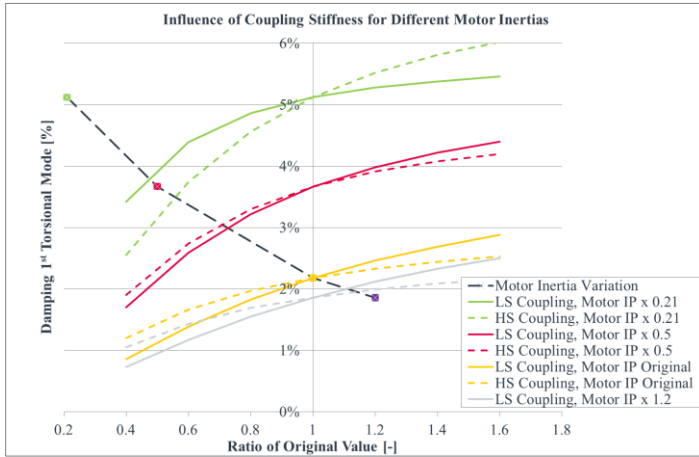


Figure 21. Variation of Coupling Stiffness and Motor Inertia

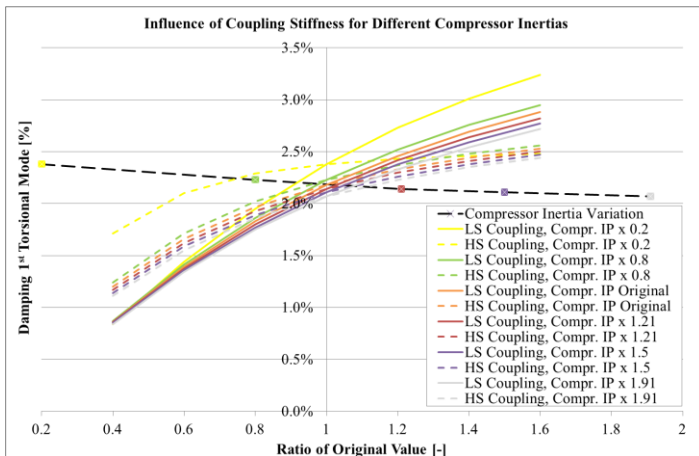


Figure 22. Variation of Coupling Stiffness and Compressor Inertia

After having identified the key influence of the motor and compressor inertia, as well as of the coupling stiffness, this intuitively leads to the conclusion, that the damping ratio can be plotted versus the 1st torsional eigenfrequency of the train.

Coupled T&L analyses were carried out for a variety of trains of different sizes. The results are shown in Figure 23. The damping ratio is plotted versus the eigenfrequency of the (pure) torsional mode. The diagram includes the results for the shaft trains A, B and C. The bearing coefficients are now based on 100% speed. This was made to get more conservative results and, further on, to have the same calculation base for trains with different eigenfrequencies. The damping ratios shown here for trains A, B and C are therefore slightly lower than shown in the previous diagrams.

Although the resulting damping ratios are not exact on a line, a clear trend is visible. The damping ratio increases with

higher eigenfrequency. Since high eigenfrequencies result for shaft trains with low motor and compressor inertia and for stiff couplings, the trend confirms the influence of these components, as already seen in Figures 21 and 22.

The second trendline (blue line) shown in the diagram includes 1% structural damping. The total damping ranges roughly from 2% to 5% and matches well with the values as known from experience.

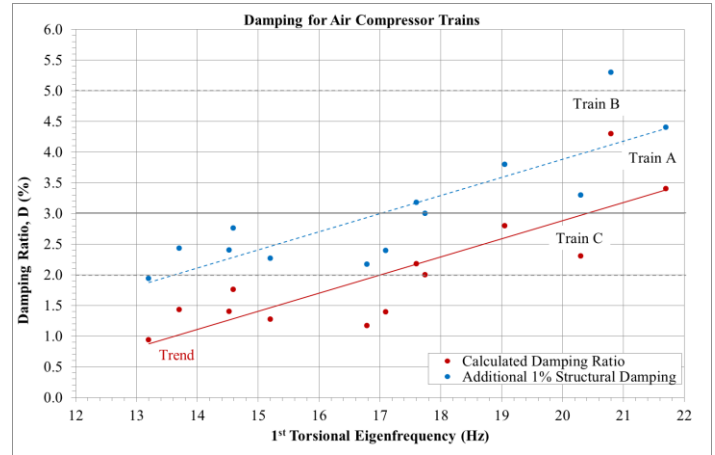


Figure 23. Influence of 1st Torsional Eigenfrequency

The diagram shown in Figure 23 is of practical interest. Herewith, the torsional modes damping can be estimated simply by knowing the eigenfrequency of the 1st mode of the torsional system.

CONCLUSIONS

The damping of the 1st torsional mode of a motor driven compressor train with gear can clearly differ from $D=3\%$, which is the authors company's standard practice for the start-up analysis of synchronous motor driven trains.

The identification of the systems damping from the shaft torques measured during the start-up of two different trains illustrated that there are non-linear effects, which can play a major role in resonance. These effects lower the torque amplitude to a higher extent, as it would be expected from the identified linear damping and, respectively, apparently further increase the total damping. However, for the measured trains, the identified linear damping was already considerably higher than the expected standard value. With the findings gained from the measurements, the implementation of torque limiting devices could be avoided.

Coupled T&L analyses were performed in terms of damped eigenvalue analyses, in order to determine the gear's contribution to the linear portion of the damping for several compressor trains of different sizes. It was observed that, depending on the actual train proportions in terms of inertia and stiffness of the components, the damping varies over a wide range. The calculations confirmed the increased damping for the measured trains. However, for certain inertia and coupling stiffness proportions, the damping was clearly lower than the standard value.

The identified key parameters, with the major influence on the damping of the 1st torsional mode, are the motor's inertia

and the torsional stiffness of the low speed coupling. The compressor's inertia and the high speed coupling play a minor role. Higher damping ratios are obtained for light motors and stiff couplings and, respectively, lower damping ratios for heavy motors and weak couplings. The eigenfrequency of the 1st torsional (uncoupled) mode was found to be a practical parameter for a rough estimation of the damping ratio in terms of a first screening of a shaft train.

The damping ratio calculated for the air compressor trains, including 1% structural damping, are within the range as known from experience.

REFERENCES

- API 617, 2002, Axial and Centrifugal Compressors and Expander-compressors for Petroleum, Chemical and Gas Industry Services, Seventh Edition, American Petroleum Institute, Washington, D.C.
- API 684, 2005, API Standard Paragraphs Rotordynamic Tutorial: Lateral Critical Speeds, Unbalance Response, Stability, Train Torsionals, and Rotor Balancing, Second Edition, American Petroleum Institute, Washington, D.C.
- Corbo, M. A., Cook, C. P., Yeiser, C. W., and Costello, M. J., 2002, Torsional Vibration Analysis and Testing of Synchronous Motor-Driven Turbomachinery, Proceedings of the Thirty-First Turbomachinery Symposium, Turbomachinery Laboratory, Texas A&M University, Texas, pp. 153-175.
- Viggiano, F., and Wattinger, W., 1994, A Torsional Damping Model for Geared Compressor Shaft Trains, Vibration in Fluid Machinery, ImechE-Seminar 1994-10, London.
- Gasch, R., Nordmann, R., and Pfützner, H., 2005, Rotordynamik, ISBN-13: 978-3540412403.
- Schmied, J., Perucchi, M., and Pradetto, J.-C., 2007, Application of MADYN 2000 to Rotordynamic Problems of Industrial Machinery, ASME Turbo Expo 2007, Montreal, Canada, Volume 5, Paper No. GT2007-27302, pp. 799-810.

ACKNOWLEDGEMENTS

The authors wish to thank all involved colleagues from MAN for the technical assistance and the precious feedback. Special thanks go to our customers for permitting to carry out the measurements and providing the support on-site.